Lissajous orbits of the equilibrium points in photogravitational elliptic restricted three body problem

Reena Kumari[1], Badam Singh Kushvah[2] and Ram Kirshna Kumar[3]

[1,2]Department of Applied Mathematics,
Indian School of Mines, Dhanbad - 826004, Jharkhand,India
[3]Department of Applied Mathematics, Nataji Subhas Institute of Technology,
Bihta-801118, Patna, India.

Abstract

We study the modified elliptic restricted three body problem introducing more massive primary as the source of radiation and the smaller primary is an oblate spheroid, which rotates around the center of mass in elliptic orbit with mean motion. Numerical as well as analytical solutions are obtained around the equilibrium point L_1, which lies between the primaries of the Sun-Jupiter system. We compute Lissajous orbits around the collinear equilibrium point L_1 in the presence of radiation pressure and oblateness. We observed that the orbital period of Lissajous orbit around L_1 is found decreased so that it takes less time to cover one period of the path.
Keywords: *ERTBP; Radiation pressure; Lissajous orbit; Oblateness*

1. Introduction

In the last decades, the elliptic restricted three body problem (ERTBP) is exceedingly important in celestial mechanics. It is one of the main mathematical models for investigations in this subject. So far as there is no general solution of the RTBP or ERTBP are known, but they have five very valuable special solutions known as Lagrangian equilibrium points. It plays a very important role in the analyses of the ERTBP and CRTBP respectively. The orbits of the celestial bodies are elliptic rather than circular, so that ERTBP can be analyze more accurately by predicting their behavior in the dynamical systems. The collinear equilibrium points play an important role for mission design, and trajectory transfers.

The ERTBP is described in considerable details by many researchers such as Danby (1964), Szebehely (1967), Broucke (1969), Sarris (1989), Zimovshchikov and Tkhai (2004), Ammar (2008), Singh and Umar (2012, 2013), Mishra et al.(2016). They have discussed the existence of equilibrium points and their stability. For modified restricted three body problem, Radzievskii (1950) discovered two out-of-plane equilibrium points L_6 and L_7; Simmons et al. (1985) showed the existence of two additional out-of-plane equilibrium points L_8 and L_9; Jiang and Yeh (2014a; 2014b) also found new equilibrium points called Jiang-Yeh points, J_{Y1}, J_{Y2}, existing on the orbital plane. Further investigations are related to Jiang-Yeh points presented in Yeh and Jiang (2016).

Nowadays, most of the researchers in recent years have focused on the Lagrangian points of the system for the mission design and transfer of trajectories Xu et al. (2007), Howell et al. (2014), Gomez et al.(2001). When the frequencies of the in-plane and out-of-plane of the equilibrium are not equal, then the orbits form Lissajous, which is a quasi-periodic orbit.

Halo orbit is a three-dimensional periodic orbits near the Lagrangian points L_1, L_2 and L_3 respectively. Farquhar was the first person who gave the name “halo orbits” after they have seen the shape from the Earth (Farquhar(1971)). It exist in many three-body systems, such as the Sun-

Earth system and the Earth-Moon system. Breakwell et al. (1979) and Howell (1984) presented the periodic halo orbits numerically and found more precise trajectories. Further, Richardson (1980) introduced a third order approximation analytical solution for halo type periodic orbit in the Sun-Earth system. The application of halo-orbits are most important for mission design. In this way, the first mission ISEE-3 was launched on August 12, 1978 in the halo orbits of the Sun-Earth system around the Lagrangian equilibrium point L_1, to study the interaction between the Earth magnetic field and solar wind. The dynamics and trajectory transfers from the Earth to halo orbit have been explained by Gomez et al . (1993), Thurman et al. (1996), Jorba et al. (1999), Koon et al. (2000).

In this study, we examine the motion of an infinitesimal body in the ERTBP when bigger primary is a source of radiation and the small primary having an oblate spheroid shape, which will contribute the effect of radiation pressure, eccentricity and oblateness respectively. On the other hand, a close attention is paid to Lissajous orbits of the Sun-Jupiter system in presence of radiation pressure and oblateness and which analyze their effects on the time period of the orbits. All computation are performed with the help of algebraic manipulator MATHEMATICA. The results are satisfactory for the collinear equilibrium point L_1 in the elliptic restricted three body system.

The present work is organized in following sections: Section 1 describes introduction. In section 2, we present the equations of motion for the elliptic restricted three body problem, whereas section 3 describes the Lissajous orbits of the system. The discussion and conclusion are drawn in section 4.

2. Equations of Motion

The elliptic restricted three body problem is a dynamical model that describes the motion of an infinitesimal body (spacecraft) under the gravitational influence of two massive bodies with masses m_1 and m_2 ($m_1 > m_2$) moving around their common center of mass in elliptical orbits with eccentricity $e \in (0, 1)$.We assume that the influence of infinitesimal mass on the motion of primaries moving under their mutual gravitational attraction is negligible. We use the standard canonical system of units, which implies that the unit of distance is the semimajor axis of the orbit of m_1 and m_2. The mass of the small primary (m_2) is given by $\mu = \frac{m_2}{m_1+m_2}$, and the mass of m_1 is $(1-\mu)$; the unit of time is taken as the time period of rotating frame moving with the mean motion (n). Hence, we have $G(m_1 + m_2) = 1$. We assume that $(-\mu, 0, 0)$ and $(1-\mu, 0, 0)$ be the coordinates of the bigger and smaller primary respectively. Also, we assume that (x, y, z) denote the coordinates of the infinitesimal body, whereas (x_1, y_1, z_1) and (x_2, y_2, z_2) be the coordinate of first and second primary body.

The equations of motion of the infinitesimal body in the rotating-pulsating coordinates system when bigger primary is taken as radiating and smaller primary having oblate spheroid are given as

$$\frac{d^2x}{df^2} - 2\frac{dy}{df} = \Omega_x, \tag{1}$$

$$\frac{d^2y}{df^2} + 2\frac{dx}{df} = \Omega_y, \tag{2}$$

$$\frac{d^2z}{df^2} = \Omega_z,$$
(3)

with the potential function

$$\Omega = \frac{1}{1+e\cos f}\left[\frac{x^2+y^2+z^2}{2}+\frac{1}{n^2}\left\{\frac{(1-\mu)q_1}{r_1}+\frac{\mu}{r_2}+\frac{\mu A_{obt}}{2r_2^3}\right\}\right],$$
(4)

and

$$r_1 = \sqrt{(x+\mu)^2+y^2+z^2}, r_2 = \sqrt{(x+\mu-1)^2+y^2+z^2}, r = \sqrt{x^2+y^2+z^2},$$
(5)

$$0 < \mu \le \frac{1}{2}, \mu = \frac{m_2}{m_1+m_2}, q_1 = 1-\frac{F_p}{F_g}, n = \sqrt{1+\frac{3}{2}A_{obt}}.$$
(6)

In the above expression, q_1 is the mass reduction factor; $n = \sqrt{1+\frac{3}{2}A_{obt}}$ is the mean motion of the elliptical orbit including oblateness with $A_{obt} = \frac{AE^2-AP^2}{5R^2}$, where AE, AP and R are respectively, the dimensional equatorial and polar radii and the effective radius of the smaller primary; m is the mass ratio of the small primary to the total mass of the primaries; r_1, r_2 are the distances of the infinitesimal mass from the bigger and smaller primaries while f and e are the true anomaly and eccentricity of the system respectively. In this work, the potential function is developed by taking into account the effect of radiation and oblateness. Now, multiplying equation (1) by $2\frac{dx}{df}$, equation (2) by $2\frac{dx}{df}$ and equation (3) by $2\frac{dz}{df}$ and adding, we get

$$2\frac{dx}{df}\frac{d^2x}{df^2}+2\frac{dy}{df}\frac{d^2y}{df^2}+2\frac{dz}{df}\frac{d^2z}{df^2} = 2\left(\frac{\partial\Omega}{dx}\frac{dx}{df}+\frac{\partial\Omega}{dy}\frac{dy}{df}+\frac{\partial\Omega}{dz}\frac{dz}{df}\right)$$
(7)

Integrating with respect to f, which gives

$$\left(\frac{dx}{df}\right)^2+\left(\frac{dy}{df}\right)^2+\left(\frac{dz}{df}\right)^2 = 2\int\left(\frac{\partial\Omega}{\partial x}dx+\frac{\partial\Omega}{\partial y}dy+\frac{\partial\Omega}{\partial z}dz\right)$$
(8)

The above expression can be written as

$$v^2 = 2\Omega - 2e\int_0^f \frac{\Omega\sin f}{1+e\cos f}df - C$$
(9)

We consider an orbit for a short time, meaning that we select the time to start for motion (say) $f = 0$. We are interested only in that part of the trajectory which takes place between $f = 0$ and $f = \in$, where $\in$ is a sufficiently smaller positive quantity. Since f is the true anomaly, this restriction amounts to consider a sufficiently small time interval, during which the primaries describe sufficiently small arcs. The second term on the right hand side of equation (9) contains the product of the eccentricity and $\in$. Consequently it is smaller than the term 2Ω. In this way, equation (9) can be approximated by

$$v^2 = 2\Omega - C, \tag{10}$$

Therefore, the zero velocity curves can be computed by

$$2\Omega' - C^* = 0. \tag{11}$$

and the variation of their shapes are governed by

$$C^* = C(1 + e\cos f). \tag{12}$$

Therefore these curves are known as the pulsating curves of zero velocity.

3. Computation of Lissajous orbit

For space missions, three dimensional equations of motion is important for geometrical reasons such as constant access to the sun for solar power or to the Earth for communications. Lissajous and halo type trajectories around the collinear equilibrium points is considered in the trajectory design of many space missions, including the Genesis mission, SOHO, ISEE-3 and many others. Halo orbits are three-dimensional periodic orbits near the equilibrium points L_1, L_2 and L_3 respectively. It consists in many restricted three-body system, such as the Sun-Earth system and the Earth-Moon system. When the in-plane and out-of-plane frequencies are such that their ratio is irrational, the projections of the motion onto the various coordinate planes produce Lissajous-type trajectories near the equilibrium points L_1, L_2 and L_3 respectively. For computation of Lissajous orbit in the rotating coordinate system, we shifted the origin of coordinates at the Lagrangian equilibrium point, and scale the variables in such a way that the distance from the smaller primary to the equilibrium point is equal to γ . Under this circumstances, we assume that the changes of coordinates is given as:

$$x = \mp\gamma_j X - \mu + a_1, y = \mp\gamma_j Y, z = \gamma_j Z, \tag{13}$$

where the upper sign corresponds to $L_{1,2}$, the lower one to L_3 , $a_1 = -1 + \gamma_1$ for $L1$, $a_1 = -1 - \gamma_2$ for L_2 and $a_1 = \gamma_3$ for L_3, and γ_j is the distance from the equilibrium point to the small primary m_2. Therefore,

$$r_1 = \sqrt{(-\gamma_j X - 1 \pm \gamma_j)^2 + \gamma_j^2 Y^2 + \gamma_j^2 Z^2}, r_2 = \sqrt{(-\gamma_j X \pm \gamma_j)^2 + \gamma_j^2 Y^2 + \gamma_j^2 Z^2}. \tag{14}$$

In order to expand the non-linear terms, we use Legendre polynomial and the following property,

$$\frac{1}{\sqrt{(x-A)^2 + (y-B)^2 + (z-C)^2}} = \frac{1}{D}\sum_{n=0}^{\infty}\left(\frac{\rho}{D}\right)^n P_n\left(\frac{Ax + By + Cz}{D\rho}\right), \tag{15}$$

where $D^2 = A^2 + B^2 + C^2, \rho^2 = x^2 + y^2 + z^2$ and P_n is the Legendre Polynomial of *nth* degree. After some computation, we obtain equations of motion which can be written as:

$$x'' - 2y' - \left(\frac{1}{1+e\cos f} + 2c_2\right)x = \frac{\partial}{\partial x}\sum_{n\geq 3}^{\infty} c_n(\mu, q_1, e, A_{obt})\rho^n P_n\left(\frac{x}{\rho}\right), \tag{16}$$

$$y'' + 2x' + \left(c_2 - \frac{1}{1+e\cos f}\right)y = \frac{\partial}{\partial y}\sum_{n\geq 3}^{\infty} c_n(\mu, q_1, e, A_{obt})\rho^n P_n\left(\frac{x}{\rho}\right), \tag{17}$$

$$z'' + c_2 z = \frac{\partial}{\partial z}\sum_{n\geq 3}^{\infty} c_n(\mu, q_1, e, A_{obt})\rho^n P_n\left(\frac{x}{\rho}\right), \tag{18}$$

where left hand side of each equation contains the linear terms, whereas the right hand side of each equation contains the non-linear terms. The coefficients c_n are given below as:

$$c_n(\mu, q_1, e, A_{obt}) = \frac{1}{\gamma_j^3(1+e\cos f)}\left[(\pm 1)^n\left(\mu + \frac{3\mu A_{obt}}{2\gamma_j^2}\right) + (-1)^n \frac{(1-\mu)q_1\gamma_j^{n+1}}{(1\mp\gamma_j)^{n+1}}\right], \; for L_j, \; j = 1, 2. \tag{19}$$

$$c_n(\mu, q_1, e, A_{obt}) = \frac{(-1)^n}{\gamma_3^3(1+e\cos f)}\left[(1-\mu)q_1 + \frac{\mu\gamma_3^{n+1}}{(1+\gamma_3)^{n+1}} + \frac{3\mu A_{obt}\gamma_3^{n+1}}{2(1+\gamma_3)^{n+1}}\right], \; for L_3 \tag{20}$$

In equations (19) and (20), we observe that in case of elliptic restricted three-body problem, the values of c_2 depends on mass parameter, radiation pressure, eccentricity and oblateness. If e = 0, $q_1 = 1$ and $A_{obt} = 0$, then the value of c_2 becomes the classical case of restricted three body problem (Jorba et al. (1999)), whereas if e = 0, $q_1 \neq 1$ and $A_{obt} \neq 0$ then the values of c_2 takes the form of Kushvah and Tiwary (2015), they have computed halo orbits in circular restricted three body problem with the effect of oblateness. The linearized equations (16) to (18) can be written as:

$$x'' - 2y' - (b_{11} + 2c_2)x = 0, \tag{21}$$

$$y'' + 2x' + (c_2 - b_{11})y = 0, \tag{22}$$

$$z'' + c_2 z = 0, \tag{23}$$

where $b_{11} = \frac{1}{1+e\cos f}$. The solution of the equation (23) is simple harmonic in z-plane, whereas the solution of the equation (21) and (22) has two real and two imaginary roots in xy-plane. The value of c_2 depends on the mass parameter μ, mass reduction factor q_1, eccentricity

e and oblateness as well as the Lagrangian points $L_i, i = 1, 2, 3$. It is not difficult to derive intervals for the values of c_2 when $\mu \in \left[0, \frac{1}{2}\right]$(Figure 1).

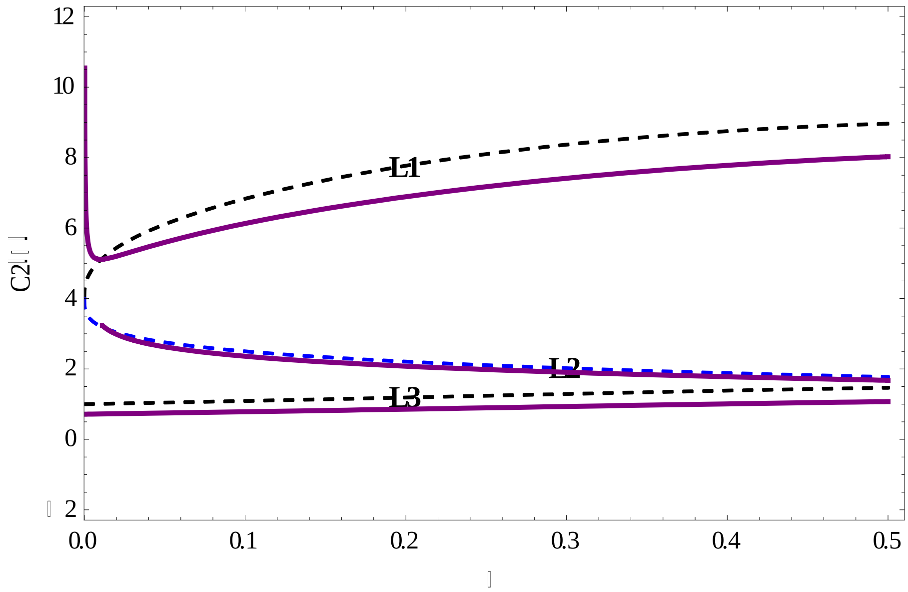

Figure1. Values of c_2 as a function of μ ($0 < \mu \le \frac{1}{2}$) for the cases $L_{1,2,3}$ in presence and absence of perturbations.

In this figure, bold line denotes the effect of perturbations, whereas light dashed line denote the classical case of elliptic restricted three body problem. Also, we observe that the position of equilibrium points is deviated due to the effect of radiation pressure and oblateness. As $c_2 > 0$ (for the three collinear points), the vertical direction is an harmonic oscillator with frequency $\nu = \sqrt{c_2}$. Also, when $\mu \in \left(0, \frac{1}{2}\right]$ we have $c_2 > \frac{1}{2}$ that forces $\omega < 0$ and $\lambda > 0$. This shows that the equilibrium point is a centre × centre × saddle (i.e., $\pm i\omega, \pm i\nu, \pm\lambda$). We replace independent variable f into t with the help of identify transformation then the solution of the linearized system is:

$$x(t) = A_1 e^{\lambda t} + A_2 e^{-\lambda t} + A_3 \cos \omega t + A_4 \sin \omega t, \quad (24)$$

$$y(t) = cA_1 e^{\lambda t} - cA_2 e^{-\lambda t} + \kappa A_3 \sin \omega t - \kappa A_4 \cos \omega t, \quad (25)$$

$$z(t) = A_5 \cos \nu t + A_6 \sin \nu t, \quad (26)$$

where $A_i, i = 1, 2...6$ are arbitrary constants, which is determined by the initial conditions. The constant value of $c, \kappa, \omega, \lambda$ and ν are depending on c_2 and b_{11} only, which are defined below:

$$\lambda = \sqrt{\frac{(c_2+2b_{11}-4)+\sqrt{9c_2^2-8c_2-16(b_{11}-1)}}{2}}, c = \frac{\lambda^2-(b_{11}+c_2)}{2\lambda}, \nu = \sqrt{c_2},$$

(27)

$$\kappa = \frac{2\omega}{\omega^2+b_{11}-c_2}, \omega = \sqrt{\frac{(4-2b_{11}-c_2)+\sqrt{9c_2^2-8c_2-16(b_{11}-1)}}{2}}.$$

(28)

It is also suitable to look at the oscillatory part of the linear solution, having an amplitude and phase,

$$x(t) = A_1 e^{\lambda t} + A_2 e^{-\lambda t} + A_x \cos(\omega t + \phi),$$

(29)

$$y(t) = cA_1 e^{\lambda t} - cA_2 e^{-\lambda t} + \kappa A_x \sin(\omega t + \phi),$$

(30)

$$z(t) = A_z \cos(\nu t + \psi),$$

(31)

where we use the relation,

$$A_3 = A_x \cos\phi, A_4 = -A_x \sin\phi, A_5 = A_z \cos\psi, A_6 = -A_z \sin\psi,$$

(32)

with A_x and A_z are the maximum in-plane and out-of-plane amplitudes of the orbit, whereas ϕ and ψ are the phases in the *xy*-plane and in the *z*-direction respectively.

We observed that when $A_1 = A_2 = 0$ are chosen in equation (29) to (31), get a periodic motion in the *xy* components together with a periodic motion in *z*-plane of a different period. This represents the Lissajous orbits in the linearized elliptic restricted three body problem. The first two components A_1 and A_2 are directly related to the unstable and stable manifold of the linear Lissajous orbit. We see that when the relation $A_1 = 0, A_2 \neq 0$, defines a stable manifold due to the backwards in time which is converges to zero. Any orbit verifying this condition will tend forward in time to the Lissajous orbit defined by A_x and A_z, because the term containing the A_2 -component in equations (24) and (25) will be zero. A similar fact happens when $A_1 \neq 0, A_2 = 0$. The term A_1 will increase in time, but become zero for backwards in time. Therefore, solutions having $A_1 \neq 0$ goes away from the oscillating or central part exponentially in forward time, and form unstable manifold.

The expression of the linearized solutions on the center manifold takes the form:

$$x(t) = -A_x \cos(\omega t + \phi),$$

(33)

$$y(t) = \kappa A_x \sin(\omega t + \phi),$$

(34)

$z(t) = A_z \cos(\nu t + \psi),$
(35)

where ω and ν are the planar and vertical characteristic frequencies and κ is a constant. The frequencies of the oscillation vary with the amplitude and for suitable amplitude, both frequencies become equal. At this point the well known halo type periodic orbit appears. When the two oscillations (that is vertical and planar) are not comparable, the motion is not periodic but it is quasi-periodic which is called Lissajous orbits. Lissajous orbit do not quite repeat after each revolution, whereas halo orbit repeat with every revolution. The linearized motion becomes quasi-periodic if the ratio of in-plane and out-of-plane are irrational.

For numerical computation of Lissajous orbit, we take the Sun-Jupiter $L1$ point and randomly chosen constant amplitude $A_x = 206000$ km and $A_z = 110000$ km. The input values of phase angles $\phi = \pi$ and $\psi = \frac{\pi}{2}$ are also used. The effect of mass reduction factor q_1 and oblateness A_{obt} of the second primary around L_1 are shown in Table 1.

Table 1. The effect of radiation pressure and oblateness around L_1.

A_{obt}	q_1	c_2	ω	λ	ν	κ	T
0.0	0.80	4.37376	2.66414	2.15463	2.09135	3.29100	2.91613
	0.85	4.43770	2.16950	2.68811	2.10658	3.31275	2.89614
	0.90	4.50164	2.18428	2.71860	2.12171	3.33436	2.87655
	0.95	4.56558	2.19895	2.73540	2.13672	3.35583	2.85736
	1.00	4.62952	2.21352	2.75874	2.15163	3.37716	2.83855
0.0025	0.80	7.20138	2.73497	3.57253	2.68354	4.14567	2.29735
	0.85	7.26532	2.74666	3.59040	2.69543	4.16297	2.28757
	0.90	7.32926	2.75830	3.60818	2.70726	4.18021	2.27792
	0.95	7.39320	2.76989	3.62588	2.71904	4.19737	2.26839
	1.00	7.45715	2.78143	3.64348	2.73078	4.21446	2.25898
0.0075	0.80	12.85660	3.62514	4.90711	3.58561	5.46873	1.73322
	0.85	12.92060	3.63396	4.92013	3.59452	5.48186	1.72902
	0.90	12.98450	3.64275	4.93311	3.60340	5.49497	1.72485
	0.95	13.04850	3.65152	4.94606	3.61226	5.50804	1.72070
	1.00	13.11240	3.66027	4.95898	3.62110	5.52108	1.71659

In this table, we observe that the frequencies on both plane of the motion increase, as we know that frequency is inversely proportional to the period, so that it takes less period to complete one path of the orbit, this happen due to the effect of perturbations. Also, we observed that the two frequencies are slightly different so that the resultant motion becomes a Lissajous orbits. Furthermore, we see that due to the effect of mass reduction factor q_1 and no effect of oblateness; numerical value of planar characteristic frequencies decrease, whereas vertical characteristic frequencies increase.

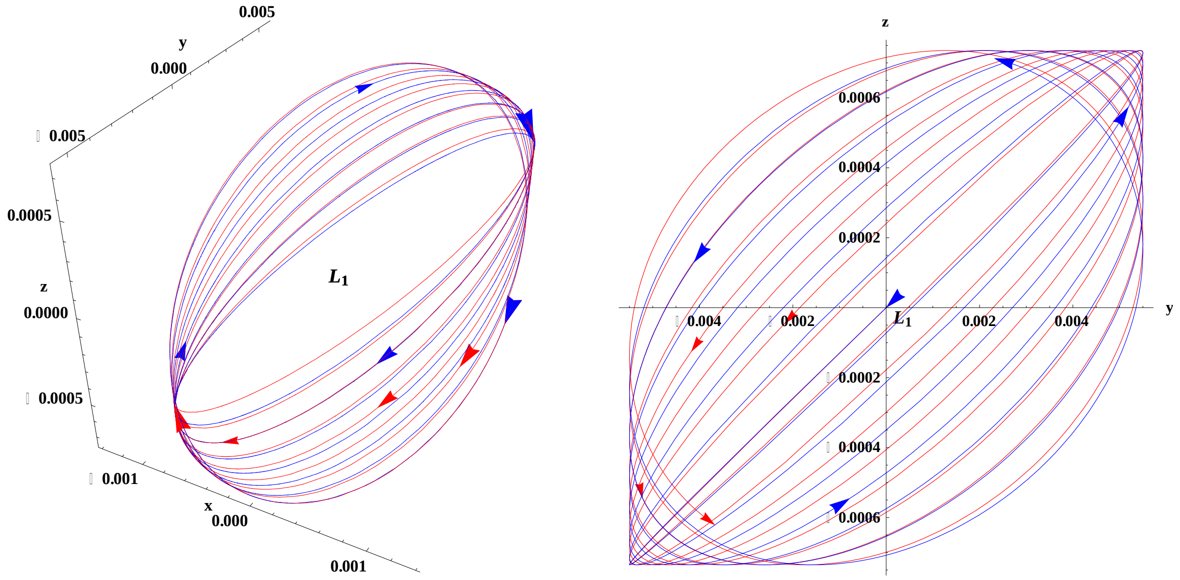

Figure 2. 3D plot and projection on yz-plane of a Lissajous orbits around L_1 in presence of radiation pressure and oblateness.

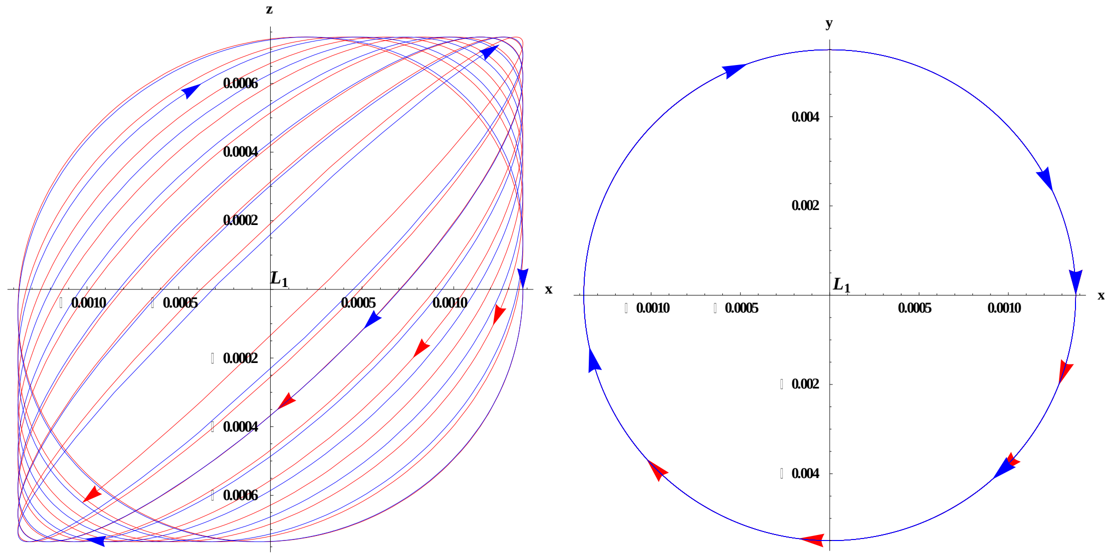

Figure 3. Projection on xz and xy-plane in presence of radiation pressure and oblateness.

The graphs of the Lissajous orbits are shown in Figure 2 and Figure 3 respectively. Left hand side of Figure 2 shows the general motion around the Lagrangian equilibrium points L_1, whereas right hand side of Figure 2 and Figure 3 shows the planar projections on *yz*, *xz* and *xy*-plane of a Lissajous trajectory. It is associated with L_1 in the Sun-Jupiter system. Blue color indicates the Lissajous orbit for classical case, whereas red color indicates that the Lissajous orbit due to the effect of perturbations in terms of radiation pressure and oblateness. Arrow indicates the clockwise direction of the motion in the *yz*, *xz* and *xy* projections. From these figures, we observe that for increasing values of oblateness coefficient A_{obt} as well as mass reduction factor q_1, time period of Lissajous orbits around L_1 takes less time to complete one period of the path of the system.

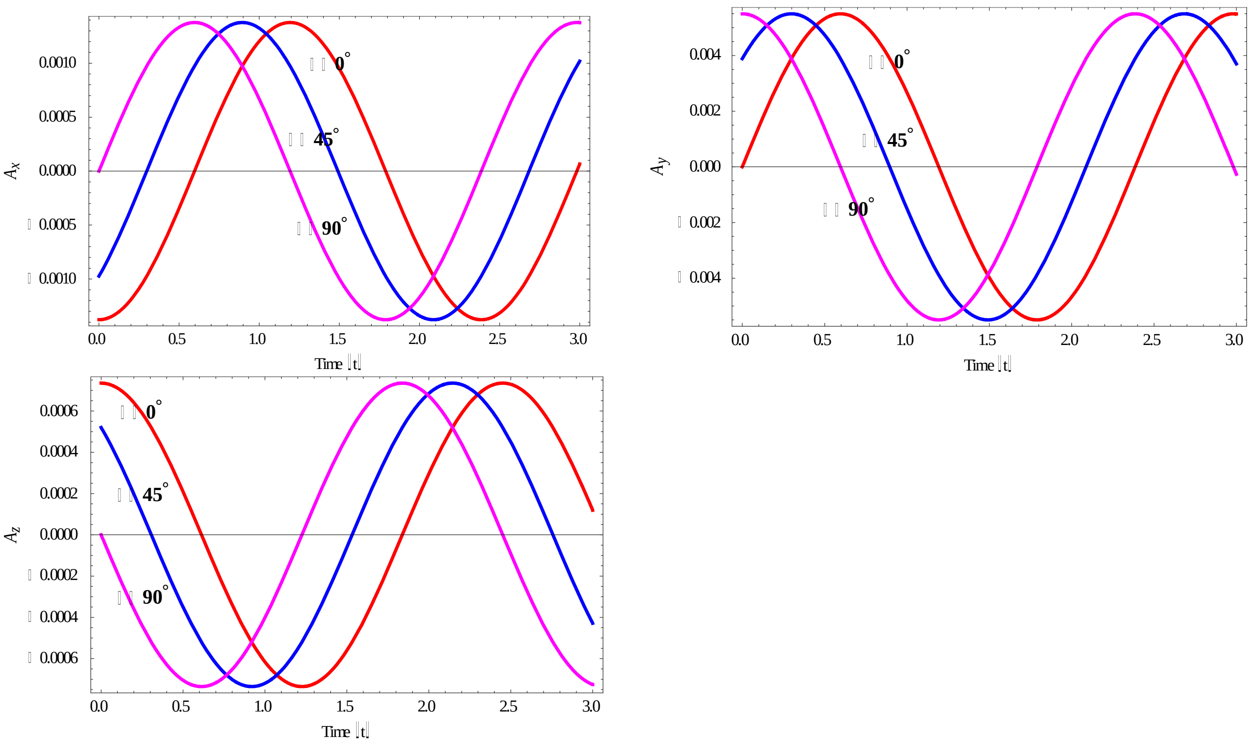

Figure 4. Relation between the amplitude A_x, A_y, A_z of the orbits and time t.

On the other hand, we also shows the graphs of amplitude verses time for different values of phase angles ϕ and ψ respectively. We observed that they maintain the differences between each another, but the nature of the amplitudes are of wave type shown in Figures 4. In this figures, we also notice that the amplitude of the Lissajous orbits are of wave types for different phase angles ϕ and ψ respectively, which represents the orbit of the system is periodic types.

4. Discussion and conclusion

We have studied elliptical restricted three problem introducing bigger primary as radiating body and smaller primary as oblate spheroid. We obtained Lissajous orbits in the neighbourhood of collinear point L_1 and found that for increasing value of mass reduction factor q_1 and oblateness coefficient A_{obt}, time period of Lissajous orbits path reduce so that it takes less time to cover one period of the path. Also, we observe that due to the effect of mass reduction factor q_1 and no effect of oblateness; numerical value of planar characteristic frequencies decrease, whereas vertical characteristic frequencies increase. The position of collinear points L_1, L_2 and L_3 are affected in presence of perturbations because it is deviated from the classical elliptic restricted three body problem joining the line of the primaries. The amplitude of the Lissajous orbits are wave types for different phase angles ϕ and ψ respectively, which represents the orbit of the system as periodic types.

Acknowledgements

We are thankful to IUCAA, Pune for partial financial support to visit library and to use computing facility.

References

*[1] M. K. Ammar, "The effect of solar radiation pressure on the Lagrangian points in the elliptic restricted three-body problem" Astrophysics and Space Science , Vol. 313, **(2008),** pp. 393–408, DOI10.1007/s10509-007-9709-z.*

*[2] J.V. Breakwell and J.V. Brown, " The 'halo' family of 3-dimensional periodic orbits in the earth-moon restricted 3-body problem", Celestial Mechanics, Vol- 20 **(1979),** pp-389–404, DOI10.1007/BF01230405.*

*[3] R. Broucke, "Stability of periodic orbits in the elliptic, restricted three-body problem", AIAA Journal, Vol. **7**, **(1969**), pp. 1003-1009, DOI 10.2514/3.5267.*

*[4] J.M.A Danby, "Stability of the triangular points in the elliptic restricted problem of three bodies", Astronomical Journal, Vol. 69, **(1964),** pp. 165, DOI 10.1086/109254.*

*[5] R.W. Farquhar, " The utilization of halo orbits in advanced lunar operations" Tech. rep., **(1971).***

*[6] G. Gomez, A. Jorba, J. Masdemont and C. Simo, " Study of the transfer from the Earth to a halo orbit around the equilibrium point L_1", Celestial Mechanics and Dynamical Astronomy , Vol. 56, **(1993**), pp. 541–562, DOI 10.1007/BF00696185.*

*[7] G. Gomez, A. Jorba, C. Simo and J. Masdemont, " Dynamics andMission Design Near Libration Points: Advanced Methods for Triangular Points. World Scientific Monograph Series in Mathematics", World Scientific Publishing Company Incorporated **(2001**), URL http://books.google.co.in/books?id=4bQknQEACAAJ.*

*[8] K.C. Howell, "Three-Dimensional Periodic Halo Orbits", Celestial Mechanics, Vol. 32, **(1984),** pp. 53.*

*[9] I.G Jiang and , L.C. Yeh, "Galaxies with supermassive binary black holes: (I) a possible model for the centers of core galaxies", Astrophysics and Space Science, Vol. 349, **(2014),**pp. 881–893, DOI 10.1007/s10509-013-1695-8.*

*[10] I.G. Jiang and L.C. Yeh, "Galaxies with supermassive binary black holes: (II) a model with cuspy galactic density profiles", Astrophysics and Space Science , Vol. 354, **(2014),** pp. 525–533, DOI 10.1007/s10509-014-2114-5.*

*[11] A . Jorba and J. Masdemont, " Dynamics in the center manifold of the collinear points of the restricted three body problem", Physica D Nonlinear Phenomena, Vol.132, (**1999**), pp. 189–213, DOI 10.1016/S0167-2789(99)00042-1.*

*[12] W.S. Koon, M.W. Lo, J.E. Marsden and S.D Ross, " Dynamical systems, the three-body problem and space mission design", International Conference on Differential Equations, **(2000),** pp. 1167–1181, World Scientific.*

*[13] V. Mishra, J. Sharma and B. Ishwar, " Stability of triangular equilibrium points in the photogravitational elliptic restricted three body problem with poynting-robertson drag", International Journal of Advanced Astronomy, Vol. 4, no. 1, **(2016),** pp. 33–38.*

*[14] V . Radzievskii, " The Restricted Problem of Three Bodies Taking Account of Light Pressure", Astronomicheskii Zhurnal, Vol. 27, (**1950),** pp. 250.*

*[15] D.L. Richardson, "Analytic construction of periodic orbits about the collinear points", Celestial Mechanics Vol.22, **(1980),** pp. 241-253, DOI 10.1007/BF01229511.*

*[16] E. Sarris, "Families of symmetric-periodic orbits in the elliptic three-dimensional restricted three-body problem", Astrophysics and Space Science, Vol. 162, **(1989)**, pp. 107-122, DOI 10.1007/BF00653348.*

*[17] J.F.L . Simmons, A.J.C. McDonald, J.C. Brown, "The restricted 3-body problem with radiation pressure", Celestial Mechanics, Vol.35, **(1985)**, pp. 145-187, DOI10.1007/BF01227667.*

*[18] J. Singh, A . Umar, " On the stability of triangular points in the elliptic R3BP under radiating and oblate primaries" Astrophysics and Space Science, Vol. 341, **(2012)**, pp. 349-358, DOI 10.1007/s10509-012-1109-3.*

*[19] J. Singh, A. Umar, "On 'out of plane' equilibrium points in the elliptic restricted three body problem with radiating and oblate primaries" Astrophysics and Space Science, Vol. 344, **(2013),** pp. 13-19 , DOI10.1007/s10509-012-1292-2.*

*[20] V. Szebehely, " Theory of Orbits: The Restricted Problem of Three Bodies", Academic Press **(1967),** URL http://books.google.co.in/books?id=sfd2QwAACAAJ.*

*[21] R.Thurman, P.A . Worfolk, " The geometry of halo orbits in the circular restricted three body Problem" Tech. rep. **(1996).***

*[22] R.D. Tiwary, B.S. Kushvah, " Computation of halo orbits in the photogravitational Sun-Earth system with oblateness", Astrophysics and Space Science Vol. 357, **(2015**), pp.73 , DOI 10.1007/s10509-015-2243-5.*

*[23] Mar Vaquero, K.C. Howell, " Design of transfer trajectories between resonant orbits in the Earth-Moon restricted problem" Acta Astronautica , Vol. 94, **(2014**), pp. 302-317, DOI10.1016/j.actaastro.2013.05.006*

*[24] R. Xu, P. Cui, D. Qiao, E. Luan, " Design and optimization of trajectory to near earth asteroid for sample return mission using gravity assists", Advances in Space Research, Vol.40, no-2, (**2007),** pp. 220 -225, DOI https://doi.org/10.1016/j.asr.2007.03.025. URL. http://www.sciencedirect.com/science/article/pii/S0273117707002517.*

*[25] L.C.Yeh, I.G . Jiang, " Galaxies with supermassive binary black holes: (III) The Roche Lobes and Jiang-Yeh Lobe in a core system", Astrophysics and Space Science, Vol. 361, **(2016),** pp. 350, DOI10.1007/s10509-016-2939-1.*

*[26] A.S. Zimovshchikov, V.N . Tkhai, " Instability of Libration Points and Resonance Phenomena in the Photogravitational Elliptic Restricted Three-Body Problem", Solar System Research , Vol. 38, **(2004),** pp. 155-164, DOI 10.1023/B:SOLS.0000022826.31475.a7.*